Short-Wave Infrared Few Cycle Pulse Generation and Characterization for High Harmonic Generation in the Water Window

Contact *adam.wyatt@stfc.ac.uk*

A. S. Wyatt, A. J. H. Jones, R. T. Chapman, C. Cacho, E. Springate

Central Laser Facility
STFC Rutherford Appleton Laboratory, OX11 0QX

P. Matía-Hernando, A. S. Johnson, D. R. Austin, J. P. Marangos, J. W. G. Tisch

Imperial College,
Blackett Laboratory, London, SW7 2AZ

Introduction

The water window (280-530eV photon energy) represents an important spectral region for spectroscopy and element specific imaging due to the relatively high transmission in water, the presence of biologically important elements such as carbon (284eV), nitrogen (410eV) and oxygen (543eV) and the potential for nanometre spatial and attosecond temporal resolutions[1]. A table-top sized source of such radiation can be realised using high harmonic generation (HHG)[2] driven by intense carrier-envelope phase (CEP) stabilized few-cycle (FC) short-wave infrared (SWIR) pulses[3] in a high pressure gas jet. Here we describe developmental progress on a collaborative project between Imperial College and the Central Laser Facility to deliver such capabilities on the Artemis laser facility.

FC-SWIR pulse generation

Millijoule-level pulses with central wavelength around 1.7μm and <50fs in duration can be generated as the idler wave in a femtosecond Ti:Sapph pumped (800nm central wavelength) optical parametric amplifier (OPA). Since the pump and seed of the OPA are derived from the same laser, and hence phase-locked, and as a direct result of the three-wave mixing process used in an OPA, the idler pulses are passively CEP stable (i.e. the phase of the electric field remains constant relative to the peak of intensity envelope for each pulse in the train). These pulses can then be spectrally broadened and temporally compressed in a hollow-core fibre (HCF) as shown in Fig. 1.

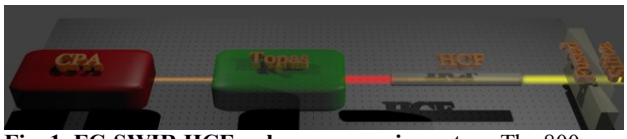

Fig. 1. FC-SWIR HCF pulse compression setup. The 800nm output from a chirped pulse amplifier (CPA) are converted to 1.7μm in a commercial OPA (Light Conversion Topas) and then spectrally broadened inside a gas filled hollow core fibre (HCF) and temporally compressed to ~10fs using anomalous dispersion in fused silica wedges.

We focused ~1mJ energy, near Fourier limited ~50fs duration SWIR pulses from a commercial OPA (Light Conversion topas) into a 400μm inner diameter hollow capillary that is differentially pumped with argon (vacuum at the entrance, 1-2bar at the exit of the fibre) with approximately 50% net transmission. Self-phase modulation (SPM) in the gas results in spectral broadening to over an octave bandwidth and approximately linear normal dispersion. After the fibre, the pulses are temporally compressed by anomalous dispersion introduced by a pair of fused silica wedges of a few millimetres in thickness. The amount of dispersion and CEP is controlled by varying the wedge insertion, and thus changing the total thickness of material.

FC-SWIR pulse characterization

Characterization of the temporal intensity after compression is an important aspect in optimization of the performance of the HCF as well as providing important information in dynamical experiments and HHG. Whilst FROG[4] and SPIDER[5] have previously been implemented in this wavelength regime, third harmonic generation (THG) dispersion scan (DS)[6] offers a much simpler configuration. Preliminary results for THG-DS in graphene at 3μm have previously been presented[7]. THG in bulk is more practical, but presents some subtle complications such as phase matching (PM) and SPM. We demonstrate THG-DS of few-cycle SWIR pulses in bulk glass and determine the effects of PM and SPM. The signal wavelength from THG of ~1100-2400nm results in a spectrum spanning ~350-800nm where silicon based detectors have high quantum efficiency, and thus is an excellent choice of non-linearity.

The THG-DS experimental setup is show in fig. 2a. A spatial mask is used to block the central portion of the beam in order to provide a background-free measurement – this was found to be extremely important due to residual THG from the OPA distorting the measured traces. The dispersion was varied by scanning the insertion of fused silica wedges and then the beam was focused into a thin glass slide (microscope cover slip) on the order of 200μm thickness. We used two different cover slips: BK7 and fused silica, in order to check the dependence of the retrieved electric field on the PM conditions. Since the third order non-linearity results in SPM and THG simultaneously, it is necessary to reduce the amount of SPM present in the pulse to prevent significant distortion of the THG spectrum. It was found that some SPM is always present and needs to be included in the DS retrieval algorithm. For example and to first order, the frequency positions of the nulls of the PM fringes shift as the intensity and thus SPM increases. Since the pulse intensity increases near the optimally compressed pulses, the PM fringes appear to "bow" around the wedge insertion position corresponding to the shortest pulse duration.

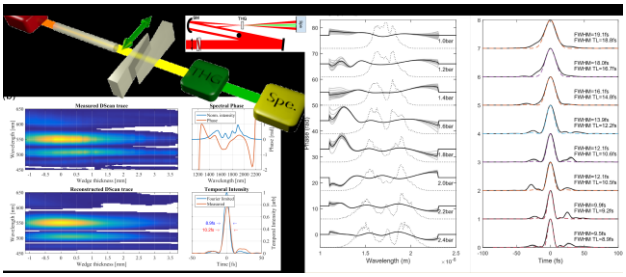

Fig. 2 THG-DS setup and results. (a) THG-DS setup. (b) Measured and reconstructed THG-DS traces (*left*) and reconstructed spectral phase/temporal intensity (*right*). Reconstructed spectral phase (c) and temporal intensity (d) as function of HCF exit gas pressure.

Fig. 2b shows measured and retrieved THG-DS traces generated in 180μm thick BK7 from a few-cycle SWIR pulse, and the corresponding reconstructed spectral phase and temporal intensity. The fringes in the DS spectrum is a result of phase mismatch between the fundamental and third harmonic fields. Figs. 2c-d plot the measured spectrum and retrieved spectral phase and temporal intensity as a function of HCF exit gas pressure ranging from 1-2.4bar. As the pressure increases, so does the spectral broadening and spectral phase oscillations with a corresponding decrease in pulse duration until the phase modulations become too severe, and thus increasing the pulse duration with further broadening. In this particular setup, the

optimum pressure was ∼2.2bar resulting in a pulse duration of ∼9fs (full width at half maximum).

High Harmonic Generation

The use of a longer wavelength (1.7μm compared to 800nm typically used) increases the ponderomotive energy as $U_p \sim \lambda^2$ and hence shifts the HHG cut-off to higher frequencies whilst simultaneously reducing the ionisation rate and thus favouring phase matching at higher pulse intensities. However, the reduced ionization also reduces the flux of the harmonic signal emitted. Driving with a few-cycle pulse reduces ionization on the leading edge, and hence allows even higher intensity pulses to be used, increasing the harmonic flux and cut-off frequency relative to a longer drive pulse duration, as well as generating a broad continuum near the cut-off frequency. CEP stabilization is required to ensure that a single half-cycle contributes to the cut-off emission with the same field strength from shot-to-shot. To maximise generation efficiency and to reach the optimal phase matching conditions, a high pressure gas jet is required, thus we developed a differentially pumped HHG gas target.

We used a ~f/25 focusing setup consisting of a Schiefspiegler telescope with silver mirrors (R_1=*0.4*m and R_2=*-1*m), a pulse energy of up to 250μJ and pulse duration ≲10fs on target. The beam waist was estimated to be ~60μm (e^{-2} radius) resulting in a peak intensity of ∼4×10^{14}W/cm^2 and hence cut-off harmonic of ∼350eV. The spatially resolved harmonic spectrum is shown in fig. 3. Since the pulses are passively CEP stable, a clear half-cycle cut-off can be observed at higher photon energies ("chevron" like structure in figure). The frequency of this cut-off is dependent on the CEP of the driving laser and can be varied by tuning the insertion of the compression wedges. Pump intensity fluctuations, alignment drift, mechanical vibrations and thermal effects results in noise and drift of the idler CEP and thus active stabilization is required to maintain absolute CEP lock. Since this has not yet been implemented, there is visible noise in the half-cycle cut-off spectrum. The dip in the harmonic spectrum around pixel 500 comes from the Cooper minimum in argon, resulting in a reduced ionization rate around 50eV.

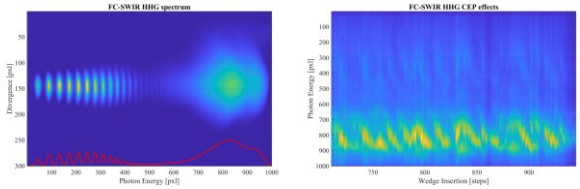

Fig. 3. HHG spectrum from few-cycle SWIR pulses. *Left*: measured HHG spectrum, continuous "chevron" pattern is a signature of attosecond pulse generation. *Right*: spatially integrated HHG spectrum as function of driving pulse CEP, noise is due to CEP drift and fluctuations.

Few-cycle SWIR OPA

The output energy of the HCF pulse compressor is limited by its transmission efficiency and maximum energy that can be coupled into the fibre. In addition, the pulse duration is limited by the higher order phase resulting from SPM and material dispersion. To overcome these issues, we propose a broadband Ti:Sapph pumped collinear OPA as shown in fig. 4.

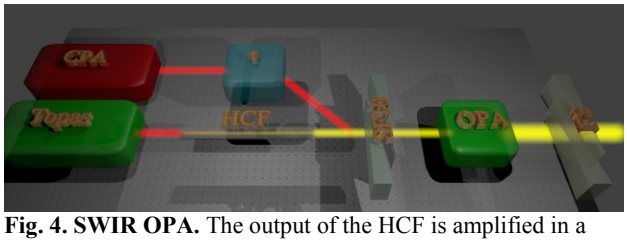

Fig. 4. SWIR OPA. The output of the HCF is amplified in a 800nm pumped OPA (Type I, 1-1.5mm thick BBO). The performance of the OPA is tuned by varying the dispersion of the seed with SF10 wedges and delay of the pump. The amplified seed is temporally compressed with fused silica (FS) wedges.

We have performed extensive numerical modelling of the performance of the OPA, as shown in fig. 5. Phase matching conditions for collinear Type I difference frequency generation near degeneracy with an 800nm pump in 1-1.5mm thick BBO allow for a very large gain bandiwdth. Since the OPA is pumped with a short pulse (<50fs) and the group velocity mismatch of the signal and idler relative to the pump have different signs, the bandwidth of the OPA is larger than that predicted by the phase matching conditions, and can potentially support over an octave of bandwidth. Due to the pump having a longer pulse duration (30-50fs) relative to the seed (∼10fs), optimum energy extraction can be realised by slightly pre-stretching the seed, achieved using SF10 wedges. We performed a numerical parameter scan as a function of SF10 wedge insertion and pump delay for a range of performance parameters. Results indicate that <7fs duration pulses are possible.

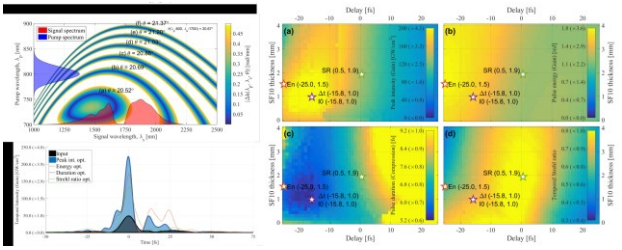

Fig. 5. SWIR-OPA modelling. *Top left*: Type I BBO phase matching conditions, pump and FC-SWIR spectra drawn overlaid for reference. *Right*: OPA performance as a function of SF10 insertion and pump delay for a range of performance parameters, (a) peak intensity, (b) pulse energy, (c) pulse duration and (d) temporal Strehl ratio (I_0/I_{FTL}). Stars mark optimal setting for each parameter. *Bottom left*: output temporal intensity for optimal performance.

We have demonstrated amplification of the octave bandwidth; fig. 6 plots measured spectra of the input and output pulses from the OPA. Also plotted for reference is the input spectrum scaled to the same energy as the output, showing the gain bandwidth supports that of the seed. In this particular setup, the input pulse energy was ∼100μJ with an output pulse energy of ∼350μJ, representing a gain of x3.5 with a pump energy of 2mJ (>10% conversion efficiency). Scaling the pump energy to ∼10mJ, we predict a pulse energy of ∼1.5mJ is possible.

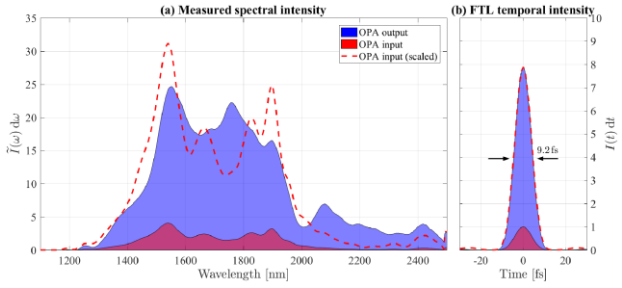

Fig. 6. SWIR OPA gain. (a) measured input and amplified seed from SWIR OPA. (b) Fourier transform limited temporal intensity of spectra plotted in (a).

100kHz upgrade

Time and angularly resolved photoelectron spectroscopy (Tr-ARPES) experiment on Artemis typically requires obtaining count statistics over several days in order to obtain sufficient signal to noise. The main limitation being the requirement to limit space-charge effects during photoionization. Acquisition

times can be significantly reduced if the repetition rate can be increased to 100kHz or more. Not only will this reduce scan durations to less than an hour, but can open up new capabilities not possible at 1kHz such as spin resolved Tr-ARPES and co-incidence measurements. Therefore the Artemis facility is currently being upgraded to 100kHz using a 200W, 1030nm picosecond pumped OPCPA system. This system is expected to deliver >170μJ energy, <30fs duration CEP stabilized pulses centred at 1.7μm, and the corresponding idler. An important question to be addressed is how to optimize the HHG for these pulses to obtain sufficient harmonic flux for pump-probe experiments, and what is the performance we could expect from such a system. We have therefore performed some initial tests using the current SWIR HCF system presented. In these tests we used an evacuated HCF to spatially filter and attenuate the topas output to give comparable parameters of the new system. We then focused these pulses into a gas jet with a 15cm lens. Using an iris both before the HCF and before the lens, the focusing geometry was varied whilst maintaining a pulse energy of 160μJ. The HHG spectrum is shown in fig. 7 for various geometries. It was found that HHG efficiency depended strongly on the focusing geometry with an optimum speed of f/20. The maximum photon energy measured was well beyond the Cooper minimum in argon, and was limited by the flat-field geometry of the system. Note also that the spectral resolution at high photon energies is not sufficient to resolve the individual harmonics, thus giving rise to the appearance of a continuous spectrum. Increasing the gas density using a needle valve resulted in an increased XUV flux. However, if the gas density was increased too much, then the spatial structure of the harmonics was significantly degraded, indicating an optimal density level.

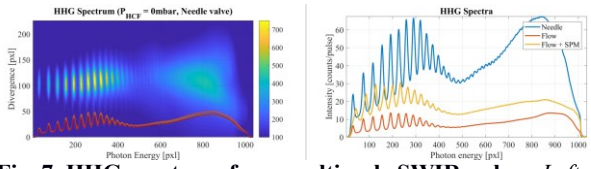

Fig. 7. HHG spectrum from multicycle SWIR pulses. *Left*: spatially resolved HHG spectrum from 160μJ energy, <50fs duration pulses centred at 1.7μm wavelength. *Right*: spatially integrated HHG spectrum under varying conditions (see text for details).

Future developments

Although the topas used to generate SWIR pulses is passively CEP stable, the CEP noise and drift can be significantly reduced by active stabilization. We therefore plan to implement an "f-2f" interferometer to directly measure the CEP phase and feed back to a piezo mirror/glass wedges inside the topas, enabling CEP sensitive measurements to be performed over longer time scales. We also have not yet performed temporal characterization or HHG with the amplified FC-SWIR pulses from the output of our octave-spanning OPA, which we plan to perform to validate our numerical modelling and demonstrate this as a practical source of high energy FC-CEP stabilized SWIR pulses. We are also designing a different configuration of our flat-field spectrometer to enable the measurement of higher photon energies in the water window and to obtain higher spectral resolution. We are currently performing experiments to calibrate the spectral axis of the flat-field spectrometers and absolute intensity of the harmonic flux.

Conclusions

We have demonstrated the generation of coherent extreme ultraviolet radiation with photon energies >150eV via HHG with <10fs duration, <250μJ energy pulses centred at 1.7μm wavelength derived from a HCF pulse compression system. Using a secondary 800nm beam, we have demonstrated amplification over the full spectrum of the few-cycle pulses with the prediction of <7fs duration, >1.5mJ energy pulses when pumped with 10mJ energy. We were able to observe a flux of >50 counts/pulse per harmonic when driven by <70fs duration, 160μJ energy SWIR pulses with modest gain on our MCP. Although the gas jet used was not optimized for this particular focusing geometry, this is a promising result and demonstrates that we expect to achieve harmonic flux sufficient for performing time-resolved photoelectron spectroscopy on the new 100kHz system.

Acknowledgements

The authors would like to thank the technical support of Phil Rice, Dave Rose and the CLF mechanical engineering department.

References

1. Francisco Silva, "Spatiotemporal isolation of attosecond soft X-ray pulses in the water window", Nat. Commun. **6**, 6611 (2015).
2. S. L. Cousin, "High-flux table-top soft x-ray source driven by sub-2-cycle, CEP stable, 1.85-μm 1-kHz pulses for carbon K-edge spectroscopy", Opt. Lett. **39**, pp. 5383-5386 (2014).
3. C Li et al, "Generation of carrier-envelope phase stabilized intense 1.5 cycle pulses at 1.75μm," Opt. Express **19**, 6783-6789 (2011).
4. X. Gu et al "Generation of carrier-envelope-phase-stable 2-cycle 740-μJ pulses at 2.1-μm carrier wavelength", Opt. Express **17**, pp. 62-69 (2009).
5. T. Witting, S. J. Weber, J. W. G. Tisch, and J. P. Marangos, "Spatio-temporal characterization of mid-infrared laser pulses with spatially encoded spectral shearing interferometry", Opt. Express **20**, pp. 27974-27980 (2012).
6. Miguel Miranda, Cord L. Arnold, Thomas Fordell, Francisco Silva, Benjamín Alonso, Rosa Weigand, Anne L'Huillier, and Helder Crespo, "Characterization of broadband few-cycle laser pulses with the d-scan technique", Opt. Express **20**, pp. 18732-18743 (2012).
7. F. Silva, M. Miranda, S. Teichmann, M. Baudish, M. Massicotte, F. Koppens, J. Biegert, and H. Crespo, "Near to mid-IR ultra-broadband third harmonic generation in multilayer graphene: few-cycle pulse measurement using THG dispersion-scan," in CLEO: 2013, OSA Technical Digest (online) (Optical Society of America, 2013), paper **CW1H.5**.